3D MODELING OF MIXTURE FORMATION AND COMBUSTION IN A DISI ENGINE AT PART-LOAD UNDER STRATIFIED OPERATION

Gustavo de Queiroz Hindi, gustavo.hindi@volvo.com
Volvo do Brasil - Curitiba - PR

Amilcar Porto Pimenta, amilcar@ita.br
ITA - Instituto Tecnológico de Aeronáutica - São José dos Campos - SP

Abstract. In the pursue for high efficiency along the whole engine operating range, light load is the most challenging situation. One of the possibilities to improve engine fuel conversion efficiency at part load is the adoption of charge stratification through direct fuel injection late in the compression stroke. The main goal is to reduce pumping loss generated from throttling by means of an overall lean mixture. An overall leaner mixture requires more air to be drawn into the cylinder to keep the mean effective pressure, thus reducing throttling losses. Also a leaner overall mixture features lower average temperatures reducing heat losses and increasing specific heat ratio. All these factors are conducive to higher fuel conversion efficiencies. To have a complete and stable combustion, cycle after cycle, in stratified operation mode is very difficult due to either the incomplete mixing in the fuel-air cloud or a too lean mixture to support flame propagation or both, may leading to excessive Unburned Hydrocarbon (UBHC) emissions. In order to assure a stable ignition and flame propagation, the fuel-air equivalence ratio near the spark plug has to be around stoichiometric at the time of spark. To assist in the design of such a complex system, numerical simulation of mixture formation and flame propagation can provide crucial information for the understanding of the combustion process. The strong coupling between fluid dynamics and chemistry makes combustion modeling a challenging task. The commercial code CONVERGE^{TM} uses Adaptive Mesh Refinement (AMR), to capture the flame brush, instead of flame surface density models. So AMR with complex chemistry for Isooctane is used to allow for a conceptual investigation of the influence of in-cylinder turbulence levels, by changing piston squish ratio, in a Direct Injection Spark Ignition (DISI) engine, at part load under stratified operation. Fuel-air equivalence ratios, flame front propagation, in-cylinder pressures and heat release rates are compared among the test cases.

Keywords: DISI, Part-load, Stratified charge, CFD

1. INTRODUCTION

In the pursue for high efficiency along the whole engine operating range, light load is the most challenging situation. With Direct Injection (DI) instead of a Port Fuel Injection (PFI) engine there exist a potential to improve cylinder to cylinder variations in fuel-air equivalence ratios, engine transient response and fuel economy (Zhao *et al.*, 1999; Kume *et al.*, 1996). One of the possibilities to improve engine fuel conversion efficiency at part load is the adoption of charge stratification through direct fuel injection late in the compression stroke. The main goal is to reduce pumping loss generated from throttling by means of an overall lean mixture. An overall leaner mixture requires more air to be drawn into the cylinder to keep the mean effective pressure, thus reducing throttling losses. Also a leaner overall mixture features lower average temperatures reducing heat losses and increasing specific heat ratio. All these factors are conducive to higher fuel conversion efficiencies.

To have a complete and stable combustion, cycle after cycle, in stratified operation mode is very difficult due to either the incomplete mixing in the fuel-air cloud or a too lean mixture to support flame propagation or both, may leading to excessive UBHC emissions. Geometric characteristics such as piston geometry, injector and spark locations, spray cone angle, penetration and mean drop sizes are important parameters (Tomoda *et al.*, 1997). On the spray side, a high tip velocity may lead to a high spray penetration, which can increase piston wall wetting without significantly improving atomization (Fraidl *et al.*, 1996). For stratified operation a more compact spray with a reduced penetration is desirable (Kume *et al.*, 1996; Ohsuga *et al.*, 1997; Wirth *et al.*, 1998). The spray also induces a secondary flow as it interacts with the in-cylinder flow which can be beneficial by increasing fuel entrainment (Kume *et al.*, 1996), but depending on the droplet sizes and in-cylinder conditions, can lead to spray contraction (Jackson *et al.*, 1997; Davy *et al.*, 1998; Kim *et al.*, 1999). Regarding the injector location, a central injection with a dominant swirl flow will tend to minimize wall wetting by concentrating the fuel-air mixture in a center position (Ohsuga *et al.*, 1997).

The injection time is an important parameter as well, as it will define the minimum time between End of Injection (EOI) and spark and also will have a role in minimizing fuel wall impingement (Kume *et al.*, 1996; Sendyka, 1998; Han *et al.*, 2002), consequently minimizing the possibility of soot formation due to wall wetting (Karl *et al.*, 1997). This time between EOI and spark has to be sufficient to allow for fuel evaporation and mixing. A too advanced injection time will tend to produce an increased spray penetration, which will spread the spray and, in general, will lead to leaner mixtures, because the time between EOI and spark will be longer increasing fuel-air mixing and fuel dispersion. A too retarded

injection time will tend to produce a reduced spray penetration, which, in general, will lead to richer mixture at spark position (Smith and Sick, 2007; Kim *et al.*, 2008).

The in-cylinder flow plays an important role where the mean flow velocity and its stability help sustaining the stratified charge and, the temporal evolution of the turbulence during compression help improving the fuel-air mixing. In order to prevent flame kernel blowout at the time of spark the mean velocity at the spark gap location cannot be excessive (Fraidl *et al.*, 1996).

Swirl as the dominant in-cylinder flow structure is important to assure a stable flame propagation, and it helps maintaining the charge stratification. Due to lower energy dissipation it can be maintained longer in the compression stroke, but as it varies with engine speed it may not be as effective for the whole engine speed range (Fraidl *et al.*, 1996; Ohsuga *et al.*, 1997; Wirth *et al.*, 1998; Jeong *et al.*, 1998). A possibility to modify the mean flow, intensifying the swirl, and thus increasing the turbulence intensity at the start of combustion is with squish. The disadvantage is that it is only effective closer to Top Dead Center (TDC). With the increase in the turbulence intensity with squish the evaporation of wall film can be more effective improving fuel-air mixture (Fraidl *et al.*, 1996).

Regarding combustion, in order to assure a stable ignition and flame propagation, the fuel-air equivalence ratio near the spark plug has to be around stoichiometric at the time of spark (Plackmann *et al.*, 1998). A fast flame initiation process with a moderate main combustion phase and with a uniform end presents, as a general rule, a good relationship among UBHC, Nitric Oxides (NOx), Break Specific Fuel Consumption (BSFC) and Coefficient of Variation (COV) of Indicated Mean Effective Pressure (IMEP) (Zhao *et al.*, 1999). The variability of Net IMEP is determined by the duration of the flame initiation process, while the efficiency is determined by the main heat release phase (Ayala *et al.*, 2006).

To assist in the design of such a complex system, numerical simulation of mixture formation and flame propagation can provide crucial information for the understanding of the combustion process. The strong coupling between fluid dynamics and chemistry makes combustion modeling a challenging task. The commercial code CONVERGE™ uses AMR, to capture the flame brush, instead of flame surface density models. So AMR with complex chemistry for isooctane is used to allow for a conceptual investigation of the influence of in-cylinder turbulence levels, by changing piston squish ratio, in a DISI engine, at part load under stratified operation. Fuel-air equivalence ratios, flame front propagation, in-cylinder pressures and heat release rates are compared among the test cases.

2. MODELING

This section summarizes the physical models used that are available in the commercial code CONVERGE™ .

2.1 Continuum phase

The method used is finite volume, with the gas phase described by the Navier-Stokes equations and the RNG $k-\epsilon$ model used for turbulence. The interpolation schemes for all transport equations is upwind, with exception of the momentum equation which is central difference. PISO is the pressure-velocity coupling algorithm used. During the whole simulation AMR is used to refine the grid with high velocity gradients, while from just prior to spark timing to the end of the simulation, it is also used to refine the grid with high temperature gradients.

2.2 Disperse phase

The Lagrangian formulation is used to describe the dispersed phase (droplet parcels), that are coupled with the continuum phase as they exchange momentum, energy and mass.

Spray Breakup Model The primary breakup is modeled using the Linearized Instability Sheet Atomization (LISA) model of Senecal *et al.* (1999) which is well suited for hollow-cone sprays. In the LISA model a three-step mechanism is used to cover the transition from the injector flow to a fully developed spray. The three-step mechanism consists of film formation, sheet breakup and final atomization.

The prediction of the drop sizes produced from primary breakup process is based on the mechanism of Dowbrowski and Johns (1963). Kevin-Helmholtz instabilities develop and grow on the film surface to a critical amplitude leading to the break off of ligaments and further into droplets.

The parcels do not interact with the gas phase till they reach their breakup length, where the Rosin-Rammler distribution is used to impose their shape diameters distribution. After this stage they are subjected to aerodynamic drag forces, evaporation, turbulent dispersion and are coupled to the gas.

The secondary breakup is modeled using Taylor-Analogy Breakup (TAB).

Droplet Drag Model As a droplet moves through a gas with large Weber number it distorts. As the drag coefficient is dependent on the droplet shape, the aerodynamic drag forces vary considerably. A classical method to calculate the drop distortion is the TAB model (Liu *et al.*, 1993). If the droplets are assumed as spherical drops, the aerodynamic drag forces are under-predicted. The dynamic drag model is then used to take in consideration the changes due to droplet distortions.

Droplet Turbulent Dispersion With the interaction of the droplets with the turbulent eddies, due to the turbulent

velocity fluctuations, there is additional diffusion. The level of interaction depends on size, mass and velocity, and may lead to a better fuel-air mixing. As part of the turbulent kinetic energy is consumed by dispersing the liquid spray droplets, the turbulence models include source terms to account for it.

Drop/Wall Interaction The liquid film transport is modeled using the film momentum equation of O'Rourke and Amsden (2000).

The possibility of rebound is evaluated for drops with low Weber numbers. Splashing is modeled in two ways, one using the approach presented by O'Rourke and Amsden (2000), and another by comparing the impinging drop Weber number to a critical splash Weber number. To create the new parcels after splashing, a fraction of the impinging drops' mass is used.

Film separation based on the criterion defined by O'Rourke and Amsden (1996) is modeled for conditions where wall film particles flow over a sharp corner. If separation occurs, the liquid film is converted to spray parcels at the edge where separation occurs with a radii equal to half the film thickness.

Evaporation The Frossling correlation (Amsden *et al.*, 1989) is used to model the time rate of change of droplet radius due to vaporization while the rate of heat conduction to the drop surface per unit area, is given by the Ranz-Marshall correlation (Baumgartem, 2006). A film temperature profile as proposed by Zeng and Lee (2000) is used to model wall film vaporization.

More details can be found in the literature (Schmidt *et al.*, 1999; Baumgartem, 2006; Richards *et al.*, 2008; Bai and Gosman, 1995).

2.3 Boundary Conditions and Engine Model

The simulated models are of a big bore 2-liter unitary cylinder displacement engine (bore = 128mm, stroke = 154mm), with a compression ratio of 14:1, 4-valve flat head, direct fuel injection with a central located pressure swirl injector and an offset spark plug (not included in the geometry) running at an engine speed of 1200 rpm.

Intake ports and valves are present in order to simulate the whole intake process. Swirl is the dominant in-cylinder flow structure induced by the intake ports' design. Exhaust ports and valves are not present and thus not simulated.

Computations are carried out from -400 deg BTDC firing, just prior to intake valve opening time, to 120 deg ATDC firing.

Spark timing is set at 15 deg BTDC.

Walls boundary conditions are no-slip and fixed temperature (450K for piston, liner and head). Inflow boundary condition with pressure of 101kPa and temperature of 363K. In-cylinder initialization does not include residuals, and has a pressure of 101kPa and a temperature of 800K.

Charge stratification is attained with Start of Injection (SOI) late in the compression stroke (75 deg BTDC) with a duration of 35 CAD.

The LISA length constant used in the sheet breakup length prediction for the onset of ligament formation, $ln(\frac{\eta_b}{\eta_0})$, that is the ratio of the wave amplitude at breakup over the initial wave amplitude is equal to 12, and the LISA size constant used for the prediction of the ligaments' diameter, C_{lisa}, is equal to 0.5.

The overall cylinder fuel air equivalence ratio is 0.43.

3. COMBUSTION MODEL WITH DETAILED CHEMISTRY

Spark ignition can be divided into three phases: breakdown, arc and glow discharge. The spark is modeled with the addition of a source term in the energy equation, resembling the usual spark ignition phases. So in the spark breakdown phase a large percentage of the total discharge energy is released in a short period, followed by the arc and glow phases.

Spark geometry is not included in the models, which makes it more prone to flame kernel blow out due to high gas velocities.

The strong coupling between fluid dynamics and chemistry makes combustion modeling a challenging task. The commercial code CONVERGE^{TM} does not employ flame surface density models to account for this interaction. With the usage of AMR, it attempts to capture the turbulent flame thickness, its transport and diffusion, due to bulk flow and turbulence, by subdividing the cells with high temperature gradients in the flame front.

The main beneficial effect of turbulence on combustion is to increase the combustion rate as the thin reaction sheet front gets wrinkled. The average distance in the flame front from the unburned to burned regions, turbulent flame thickness, in a spark-ignition engines is in the order of millimeters, while the laminar flame thickness can be in the order of 0.01mm (Ziegler *et al.*, 1988; Heywood, 1988, 1994). It is worth noting that there is no turbulent enhancement of the chemical kinetics.

The flame regime is going to be verified analytically, in the results part of this document, by calculating the non-dimensional numbers that characterize the interaction between turbulence and chemistry.

The SAGE chemical kinetics solver from Senecal *et al.* (2003) is used to resolve the oxidation mechanism for Isooctane from Jia and Xie (2006) consisting of 38 species and 69 elementary reactions that is used in this work.

4. RESULTS

This work is split in two main parts that will be described below. Also the mesh independence study and the combustion regime analytical verification are presented.

4.1 Mesh Independence Study

In this work a grid independence regarding refinement level was performed for the final geometry tested, considering minimum cell sizes of 0.125mm and 0.25mm in the high temperature gradient region "Fig. 1". As can be seen from the assessment line A, extracting points through the flame front, a maximum temperature difference between grids of 11% has been found. So as good agreement was achieved with both cell refiments, to minimize computational costs, a minimum cell size of 0.25mm was used in the AMR.
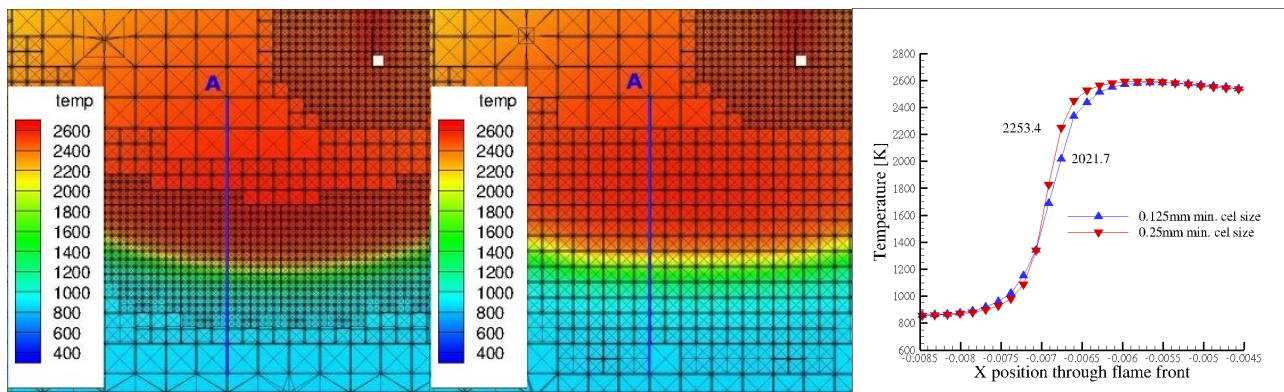
a. 0.125mm min. grid size   b. 0.25mm min. grid size   c. Temperatures through flame front cut

Figure 1. Flame front showing two levels of refiment

4.2 Part I

To assess mixture formation and combustion progress trying to isolate only the impact of squish ratio, a set of 3 piston geometries with same squish height (2mm), but different squish ratios (0.5, 0.6 and 0.7) have been evaluated "Fig. 2". Piston bowl angles are kept constant among geometries with changing depths as a consequence of a constant compression ratio.
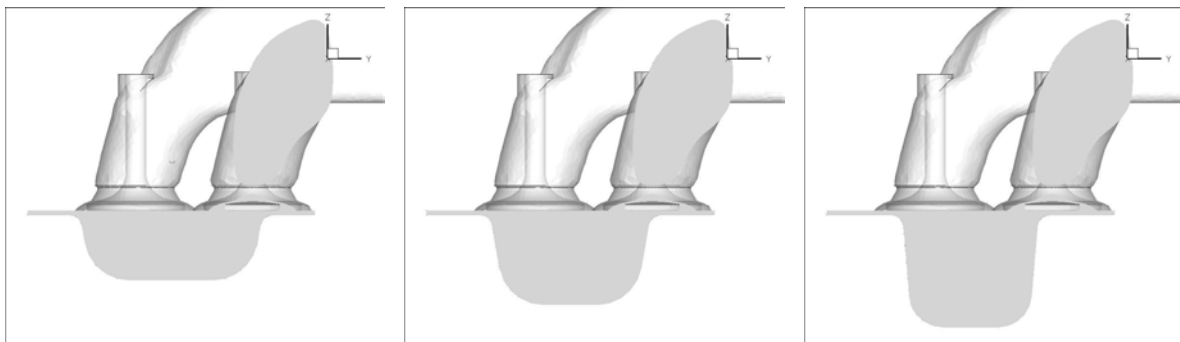
Figure 2. Piston bowl geometries - Squish ratios 0.5, 0.6 and 0.7 respectively

The influence of the squish ratio in the Turbulence Kinetic Energy (TKE) can be seen in "Fig. 3", showing a small increase in the domain at spark timing (15deg BTDC).

The mass averaged TKE and TKE dissipation versus crank angle can be seen in "Fig. 4". There is a 10% increase in TKE at spark timing, and a 29% increase at TDC firing for squish 0.7 over squish 0.5. The increase in TKE after TDC firing with squish ratio 0.6, is due to the combustion induced turbulence. As will be shown later, the other geometries have not presented a favorable scenario for combustion to proceed after spark initiation.

The velocity vectors showing the swirl structure, at spark timing and at spark location, as seen in "Fig. 5" shows, as expected, to be stronger for higher squish ratios, but also as a consequence of a reduction in bowl diameter with increasing squish ratio.

Swirl ratio close to TDC can be seen in "Fig. 6".

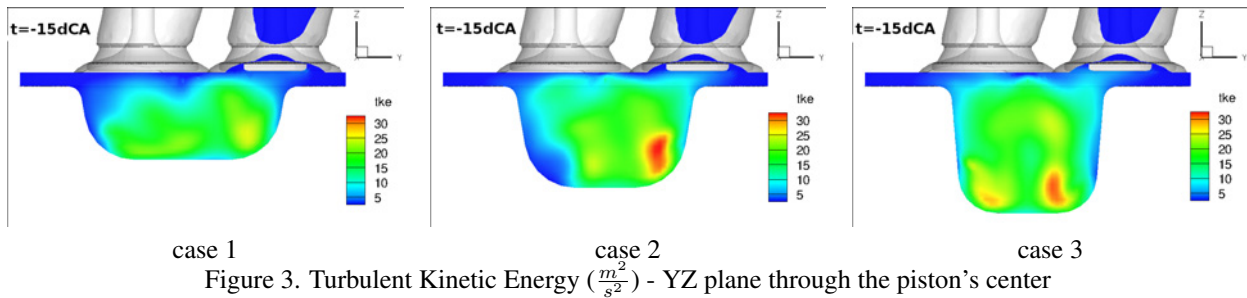case 1   case 2   case 3

Figure 3. Turbulent Kinetic Energy ($\frac{m^2}{s^2}$) - YZ plane through the piston's center

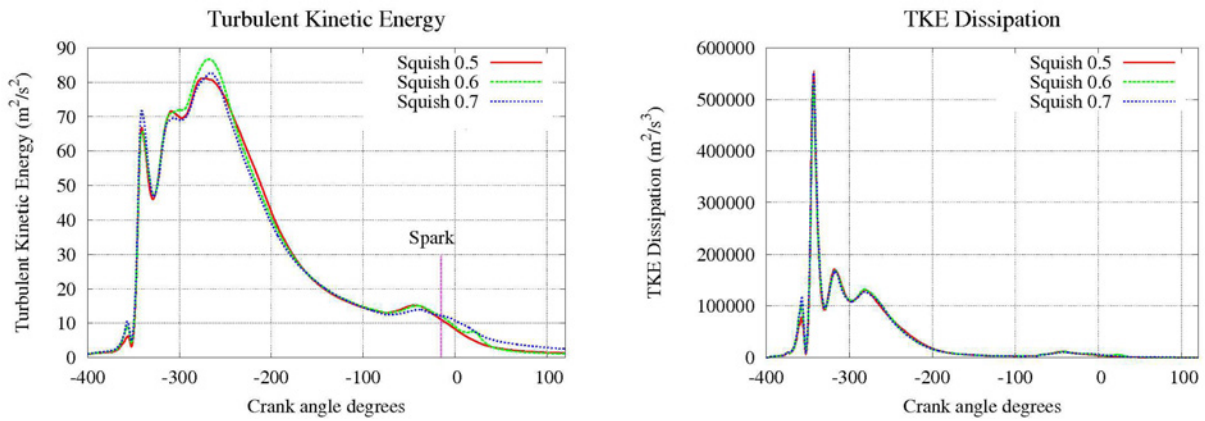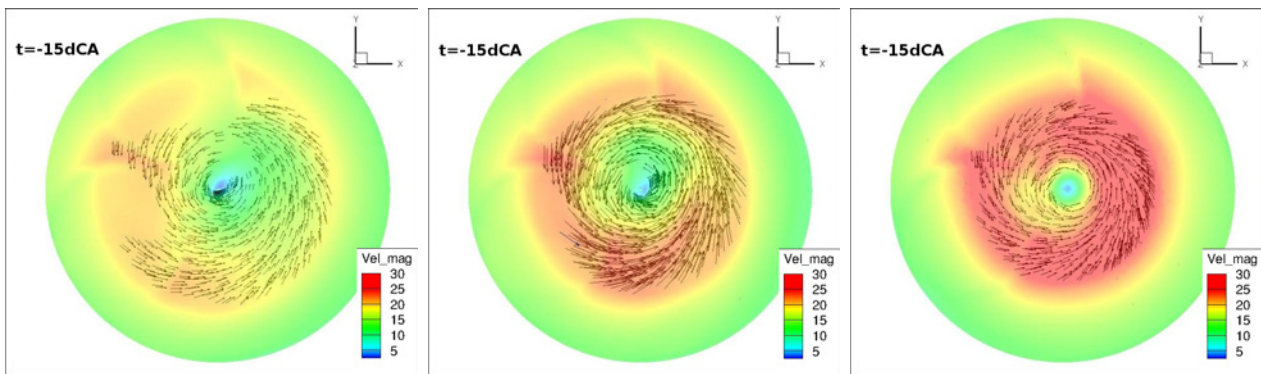Figure 4. Turbulent Kinetic Energy and TKE Dissipation

case 1   case 2   case 3

Figure 5. Velocity magnitude ($\frac{m}{s}$) - XY plane at spark position height at spark timing

As can be seen in "Fig. 7" there is not a big influence of the turbulence, due to turbulent dispersion, in the droplets size reduction.
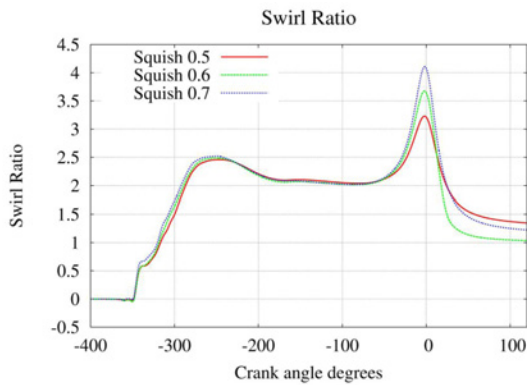
Figure 6. Swirl ratio
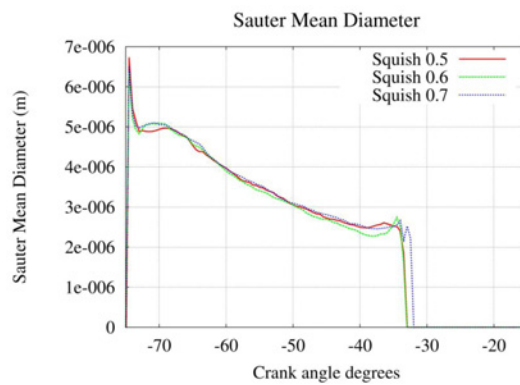
Figure 7. Sauter Mean Diameter

The fuel air equivalence ratio, ϕ, at 55, 35 and 15 deg BTDC respectively can be viewed in "Fig. 8", "Fig. 9", "Fig. 10".

The in-cylinder flow structure causes the fuel spray to be off centered.
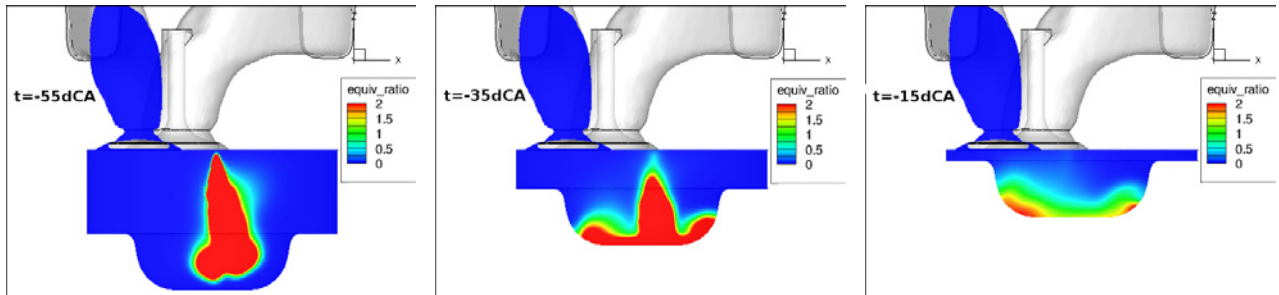

Figure 8. Fuel Air Equivalence Ratio - Squish ratio 0.5 - XZ plane through the piston's center
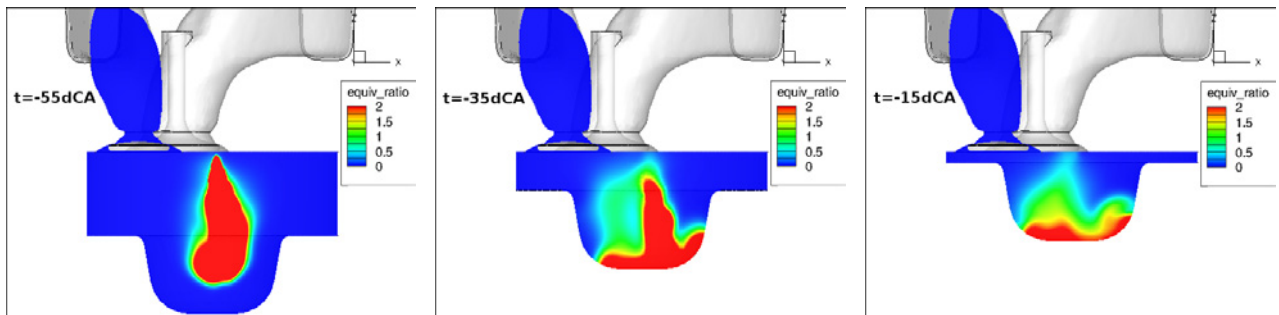

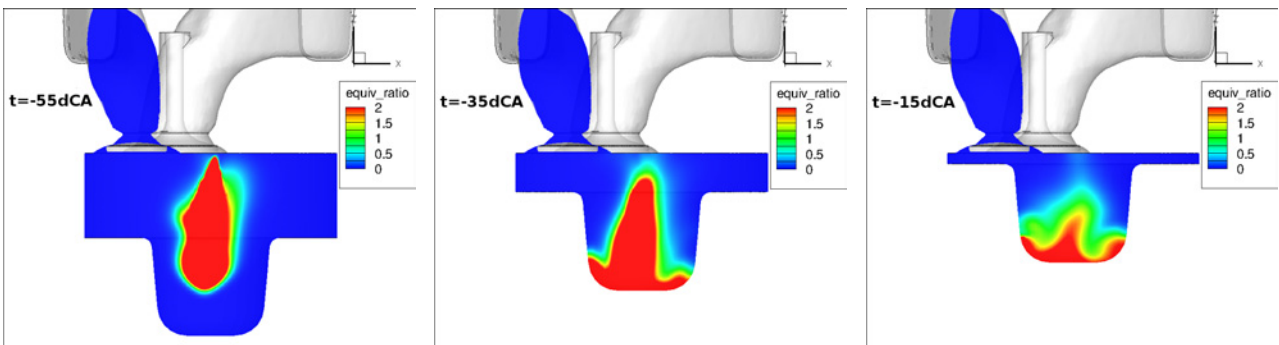Figure 9. Fuel Air Equivalence Ratio - Squish ratio 0.6 - XZ plane through the piston's center

Figure 10. Fuel Air Equivalence Ratio - Squish ratio 0.7 - XZ plane through the piston's center

As a consequence of the fuel air equivalence ratio, at spark timing, there is not a condition for flame initiation and propagation for cases with squish ratio 0.5 and 0.7. This is not related to the squish ratio itself, but due to the excessive deep bowl for the case with squish ratio 0.7, and due to the wider bowl for the case with squish ratio 0.5, as a consequence of the same compression ratio and similar bowl shapes.The flame propagation for the case with squish ratio of 0.6 can be seen in "Fig. 11", "Fig. 12", at TDC, 15 and 30 deg ATDC, respectively.
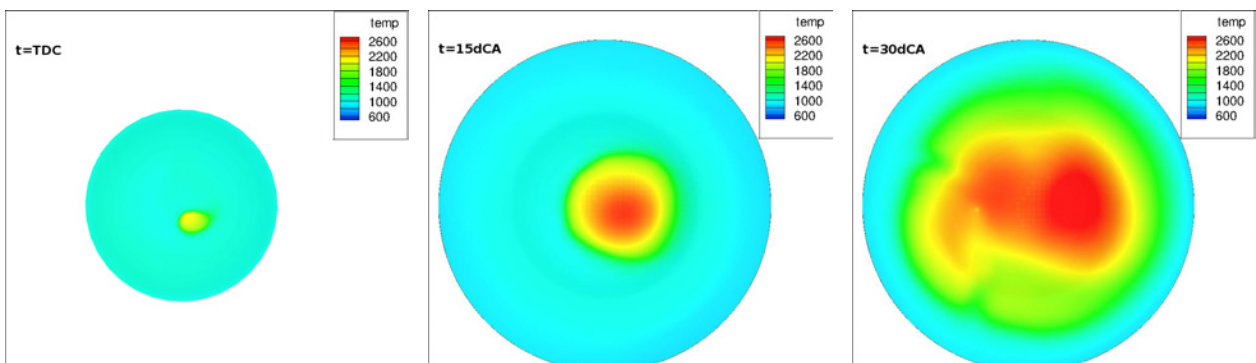

Figure 11. Upper view of flame propagation - XY plane at spark position height
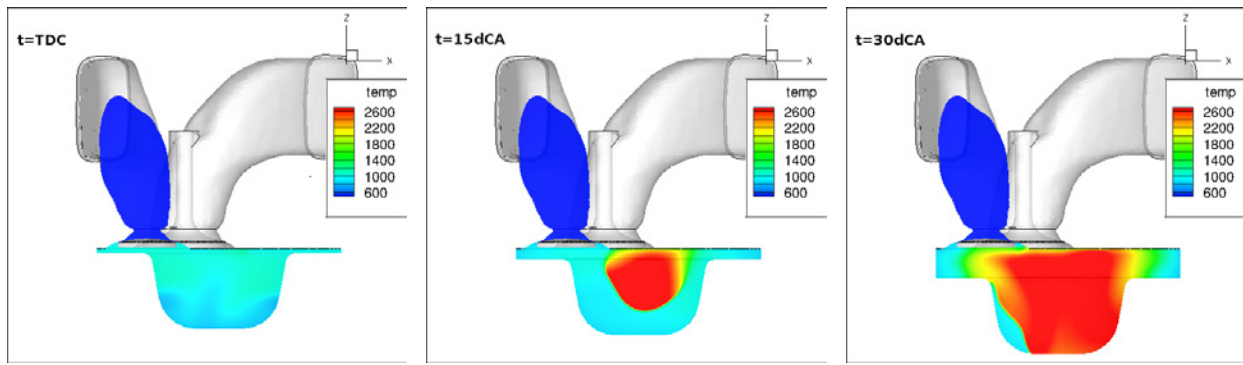
Figure 12. Side view of flame propagation - XZ plane at piston's center

As can be seen from "Fig. 13", the combustion process is very slow and leads to a double peak in mean cylinder pressure.
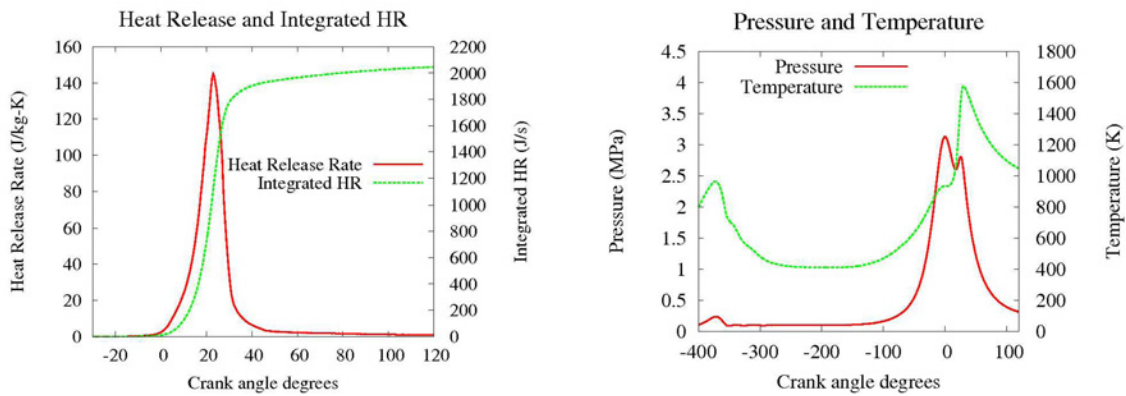

Figure 13. HRR, Integrated HR, Pressure and Temperature

4.3 Part II

To assess a set of observations made with these 3 initial geometries, like TKE increase with squish ratio increase, the squish ratio of 0.7 is desired. To have the fuel plume closer to the spark location, a reduced bowl depth is desired. To create a flow structure to advect the fuel towards the spark plug and try to centralize the fuel spray, additional features in the bottom of the piston bowl seems to be required. So a fourth piston bowl with squish height of 2mm, squish ratio of 0.7 but with a shallower bowl, and additional features in the bottom of the bowl, has been evaluated "Fig. 14".
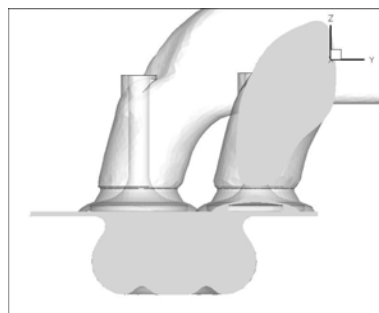

Figure 14. 4th piston geometry - Squish ratio 0.7 and shallow bowl

Φ contour plots, at 55, 35 and 15 deg BTDC respectively, can be seen in "Fig. 15", showing that a centralized fuel plume is attained with this new geometry.

Flame propagation, at TDC, 15 and 30 deg ATDC respectively can be seen in "Fig. 16","Fig. 17", showing that a more centered and faster combustion is attained, as fuel is been continuously advected towards the flame front.

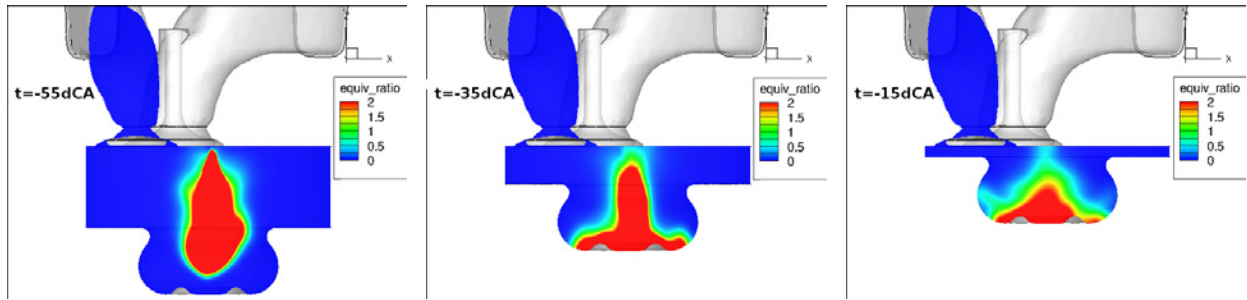This faster combustion can also be seen from "Fig. 18".

Figure 15. Fuel Air Equivalence Ratio - XZ plane through the piston's center
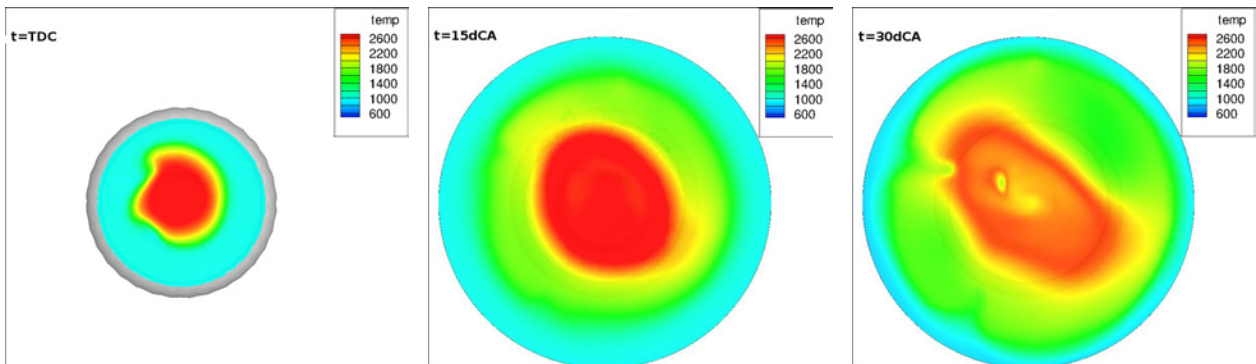

Figure 16. Upper view of flame propagation - New piston geometry - XY plane at spark position height
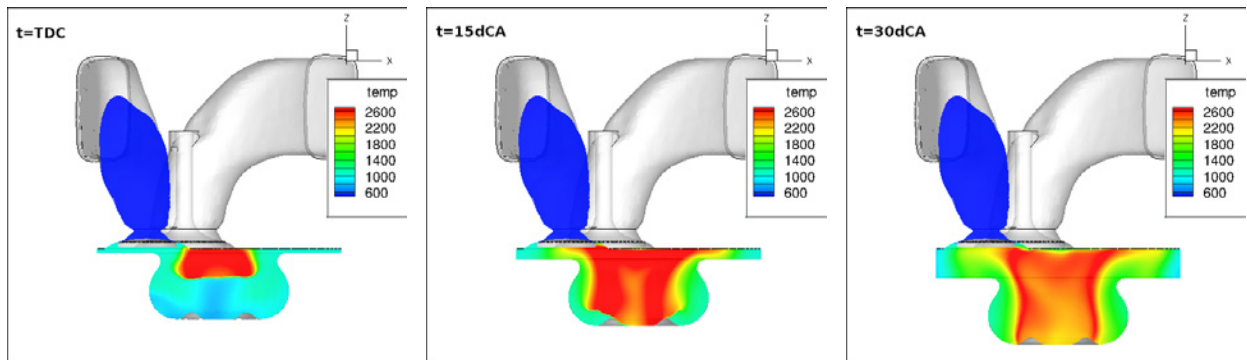

Figure 17. Side view of flame propagation - New piston geometry - XZ plane at piston's center
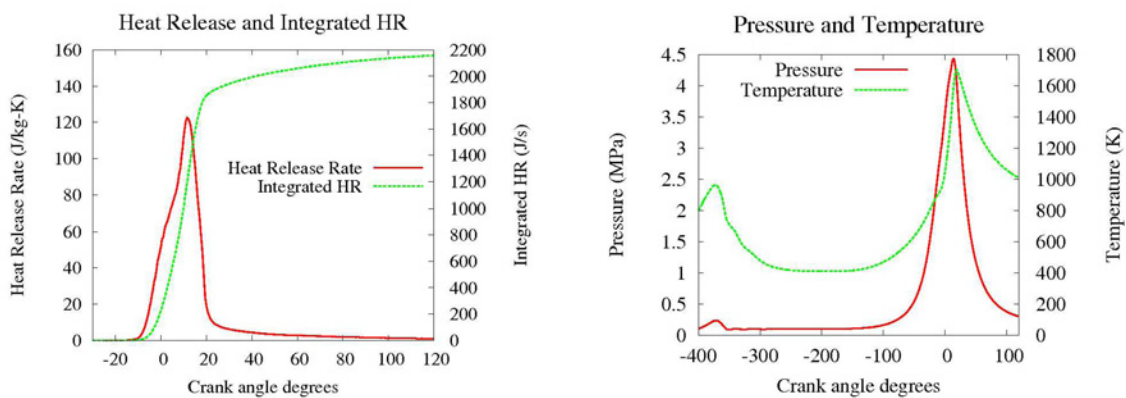

Figure 18. HRR, Integrated HR, Pressure and Temperature - New piston geometry

4.4 Combustion Regime Analytical Verification

To verify the combustion regime assumption, the non-dimensional numbers that characterize it are calculated analytically at TDC for the last piston geometry tested.

Calculating the Damköhler number, that is the ratio of the integral time scale to the chemical time scale per "Eq. (1)".

$$D_a = \frac{\tau_t}{\tau_c} = \frac{\frac{l_t}{u'}}{\frac{\delta}{S_L^0}} = 103.3 \tag{1}$$

The Karlovitz number, that is the ratio of the chemical time scale to the Kolmogorov time scale per "Eq. (2)".

$$K_a = \frac{\tau_c}{\tau_k} = \frac{\frac{u'}{\eta_k}}{\frac{S_L^0}{\delta}} = 0.1 \tag{2}$$

The turbulence Reynolds number, based on the integral length scale per "Eq. (3)".

$$Re_t = \frac{u' * l_t}{\nu} = 166.2 \tag{3}$$

These numbers show that the chemical time scales are shorter than either the integral turbulence time scale ($D_a >> 1$), or the Kolmogorov time scale ($K_a < 1$), which confirms the flamelet regime.

5. CONCLUSIONS

This work has shown how numerical simulation can assist in the preliminary design of a system with such level of complex interactions between spray, in-cylinder flow structures and combustion. It can be used to provide understanding of the involved phenomena, and easily evaluate various solutions.

The attempt to isolate the squish ratio, maintaining the bowl shape, for the evaluated cases in part I have led to a scenario not more appropriate for flame initiation and propagation for 2 of the 3 geometries.

The observations made during part I of the work, have led to the proposal of a fourth geometry to improve the mixture formation and combustion process. As can be seen comparing "Fig. 13" and "Fig. 18" the combustion process was about 12 deg faster with the piston proposed in part II of this work.

6. ACKNOWLEDGEMENTS

7. REFERENCES

Amsden, A.A., O'Rourke, P.J. and Butler, T.D., 1989. "Kiva-ii: A computer program for chemically reactive flows with sprays". *Los Alamos National Laboratory Report No. LA-11560-MS*.

Ayala, F.A., Gerty, M.D. and Heywood, J.B., 2006. "Effects of combustion phasing, relative air-fuel ratio, compression ratio, and load on si engine efficiency". *SAE Paper No. 2006-01-0229*.

Bai, C. and Gosman, A.D., 1995. "Development of methodology for spray impingement simulation". *SAE Paper No. 950283*.

Baumgartem, C., 2006. *Mixture Formation in Internal Combustion Engines*. Springer-Verlag.

Davy, M.H., Williams, P.A. and Anderson, R.W., 1998. "Effects of injection timing on liquid-phase fuel distributions in a centrally-injected four-valve direct-injection spark-ignition engine". *SAE Paper No. 982699*.

Dowbrowski, N. and Johns, W.R., 1963. "The aerodynamic instability and disintegration of viscous liquid sheets". *Chemical Engineering Science*, Vol. 18(3), pp. 203–214.

Fraidl, G.K., Piock, W.F. and Wirth, M., 1996. "Gasoline direct injection: Actual trends and future strategies for injection and combustion systems". *SAE Paper No. 960465*.

Han, Z., Li, J. and Trigui, N., 2002. "Stratified mixture formation and piston surface wetting in a disi engine". *SAE Paper No. 2002-01-2655*.

Heywood, J.B., 1988. *Internal Combustion Engine Fundamentals*. McGraw-Hill Book Company.

Heywood, J.B., 1994. "Combustion and its modeling in spark-ignition engines". *International Symposium COMODIA*.

Jackson, N.S., Stokes, J., Whiteker, P.A. and Lake, T.H., 1997. "Stratified and homogeneous charge operation for the direct injection gasoline engine - high power with low fuel consumption and emissions". *SAE Paper No. 970543*.

Jeong, K.S., Ohm, Y., Yoon, Y. and Jeung, I.S., 1998. "Initial flame development under fuel stratified conditions". *SAE Paper No. 981429*.

Jia, M. and Xie, M., 2006. "A chemical kinetics model of iso-octane oxidation for hcci engines". *Fuel*, Vol. 85(17-18), pp. 2593–2604.

Karl, G., Kemmler, R., Bargende, M. and Abthoff, J., 1997. "Analysis of a direc injected gasoline engine". *SAE Paper No. 970624*.

Kim, S.J., Kim, Y.N. and Lee, J.H., 2008. "Analysis of the in-cylinder flow, mixture formation and combustion processes in a spray-guided gdi engine". *SAE Paper No. 2008-01-0142*.

Kim, Y.J., Lee, S.H. and Cho, N.H., 1999. "Effects of air motion on fuel spray characteristics in a gasoline direct injection engine". *SAE Paper No. 1999-01-0177*.

Kume, T., Iwamoto, Y., Iida, K., Murakami, M., Akishino, K. and Ando, H., 1996. "Combustion control technologies for direct injection si engine". *SAE Paper No. 960600*.

Liu, A.B., Mather, D.K. and Reitz, R.D., 1993. "Modeling the effects of drop drag and breakup on fuel sprays". *SAE Paper No. 930072*.

Ohsuga, M., Shiraishi, T., Nogi, T., Nakayama, Y. and Sukegawa, Y., 1997. "Mixture preparation for direct-injection si engines". *SAE Paper No. 970542*.

O'Rourke, P.J. and Amsden, A.A., 1996. "A particle numerical model for wall film dynamics in port-injected engines". *SAE Paper No. 961961*.

O'Rourke, P.J. and Amsden, A.A., 2000. "Spray/wall interaction submodel for the kiva-3 wall film model". *SAE Paper No. 2000-01-0271*.

Plackmann, J.D., Kim, T. and Ghandhi, J.B., 1998. "The effects of mixture stratification on combustion in a constant-volume combustion vessel". *SAE Paper No. 980159*.

Richards, K.J., Senecal, P.K. and Pomraning, E., 2008. "Converge^{TM} (version 1.3)". *Convergent Science, Inc, Middleton, WI*.

Schmidt, D.P., Nouar, I., Senecal, P.K., j Hoffman, Rutland, C.J., Martin, J. and Reitz, R.D., 1999. "Pressure-swirl atomization in the near field". *SAE Paper No. 1999-01-0496*.

Sendyka, B., 1998. "A description of the shape of an air-fuel mixture and determination of injection advance angles related to the spark discharges in a gasoline direct injection engine". *SAE Paper No. 980496*.

Senecal, P.K., Pomraning, E., Richards, K.J., Briggs, T.E., Choi, C.Y., MacDavid, R.M. and Patterson, M.A., 2003. "Multi-dimensional modeling of direct-injection diesel spray liquid length and flame lift-off length using cfd and parallel detailed chemistry". *SAE Paper No. 2003-01-1043*.

Senecal, P.K., Schmidt, D.P., Nouar, I., Rutland, C.J., Reitz, R.D. and Corradini, M.L., 1999. "Modeling high-speed viscous liquid sheet atomization". *International Journal of Multiphase Flow*, Vol. 25(6-7), pp. 1073–1097.

Smith, J. and Sick, V., 2007. "The prospects of using alcohol-based fuels in stratified-charge spark-ignition engines". *SAE Paper No. 2007-01-4034*.

Tomoda, T., Sasaki, S. and Sawada, D., 1997. "Development of direct injection gasoline engine - study of stratified mixture formation". *SAE Paper No. 970539*.

Wirth, M., Piock, W.F., Fraidl, G.K., Schoeggl, P. and Winklhofer, E., 1998. "Gasoline di engines: The complete system approach by interaction of advanced development tools". *SAE Paper No. 980492*.

Zeng and Lee, C.F., 2000. "Multicomponent fuel fil vaporization model for multidimensional computations". *Journal of Propulsion and Power*, Vol. 16(6), pp. 964–973.

Zhao, F., Lai, M.C. and Harrington, D.L., 1999. "Automotive spark-ignited direct-injection gasoline engines". *Progress in Energy and Combustion Science*, Vol. 25(5), pp. 437–562.

Ziegler, G.F.W., Zettlitz, A., Meinhardt, P., Herweg, R., Maly, R. and Pfister, W., 1988. "Cycle-resolved two-dimentional flame visualization in a spark-ignition engine". *SAE Paper No. 881634*.

8. Responsibility notice

The author(s) is (are) the only responsible for the printed material included in this paper